HHS Public Access

Author manuscript

Nano Lett. Author manuscript; available in PMC 2017 January 13.

Published in final edited form as:

Nano Lett. 2016 January 13; 16(1): 721–727. doi:10.1021/acs.nanolett.5b04549.

Highly Stretchable Fully-Printed CNT-based Electrochemical Sensors and Biofuel Cells: Combining Intrinsic and Design-induced Stretchability

Amay J. Bandodkar[#], **Itthipon Jeerapan**[#], **Jung-Min You**, **Rogelio Nuñez-Flores**, and **Joseph Wang**[*]

Department of NanoEngineering, University of California San Diego, La Jolla, CA 92093, USA

Abstract

We present the first example of an all-printed, inexpensive, highly stretchable CNT-based electrochemical sensor and biofuel cell array. The synergistic effect of utilizing specially tailored screen printable stretchable inks that combine the attractive electrical and mechanical properties of CNTs with the elastomeric properties of polyurethane as a binder along with a judiciously designed free-standing serpentine pattern enables the printed device to possess two degrees of stretchability. Owing to these synergistic design and nanomaterial-based ink effects, the device withstands extremely large levels of strains (upto 500% strain) with negligible effect on its structural integrity and performance. This represents the highest stretchability offered by a printed device reported to date. Extensive electrochemical characterization of the printed device reveal that repeated stretching, torsional twisting and indenting stress has negligible impact on its electrochemical properties. The wide-range applicability of this platform to realize highly stretchable CNT-based electrochemical sensors and biofuel cells has been demonstrated by fabricating and characterizing potentiometric ammonium sensor, amperometric enzyme-based glucose sensor, enzymatic glucose biofuel cell and self-powered biosensor. Highly stretchable printable multi-analyte sensor, multi-fuel biofuel cell or any combination thereof can thus be realized using the printed CNT array. Such combination of intrinsically-stretchable printed nanomaterial-based electrodes and strain-enduring design patterns holds considerable promise for creating an attractive class of inexpensive multi-functional, highly stretchable printed devices that satisfy the requirements of diverse healthcare and energy fields wherein resilience towards extreme mechanical deformations is mandatory.

Keywords

Printed electronics; electrochemical sensors; carbon nanotubes; biofuel cells; stretchable devices

[*]josephwang@eng.ucsd.edu; Fax: +1 (858) 534 9553; Tel: +1 (858) 246 0128.

[#]Equal Contribution

Supporting Information

Materials, methods, video and figures. This material is available free of charge via the Internet at http://pubs.acs.org.

The authors declare no competing financial interest.

The past decade has witnessed an exponential increase in research activities related to soft, stretchable electronics.[1,2] These devices readily yield to external stress and thus survive mechanical deformations with minimal effect on their performance. This remarkable behavior has led to a foray of stretchable electronics in diverse fields that were originally untouched by conventional rigid electronics, for example, wearable devices,[3–5] robotics,[6,7] or bionics,[8,9] which demand electronics that can endure external strain. Diligent engineering of fabrication materials and of the device design is an indispensable requisite for achieving devices that are compliant towards extreme stress.[10] Keeping cognizance of this critical requirement, researchers have developed stretchable devices that rely on serpentine metallic structures,[11] nanomaterials,[12,13] conductive polymers,[14,15] or liquid metals.[16] Although such ingenious approaches have led to compliant soft electronics, they rely on expensive lithographic techniques[17] or small-scale spin/spray coating methods[18] that lead to high manufacturing costs. Alternatively, screen printing techniques offer low-cost and large-scale fabrication of reproducible printed devices.[19] The present work leverages screen printing process coupling specially engineered stretchable inks and a careful device design pattern to realize highly stretchable carbon nanotube (CNT)-based electrochemical devices that can withstand extreme strains up to 500% with minimal effect on their performance.

Printed electronics has acquired tremendous attention and its market size is expected to reach $300 billion over the next two decades.[20] Printed electrochemical devices, in particular, are an important section of printed electronics that plays a pivotal role in healthcare,[21] energy[22] and security[23] domains. However, majority of these printed electrochemical high-performance devices are mechanically fragile. In many of these applications, the printed electrochemical devices experience harsh mechanical deformations that hamper full realization of their potential. In order to address this drawback, researchers have introduced printed electrochemical devices based on flexible paper,[24] plastic[25,26] or textiles.[27,28] Recently, we demonstrated a stretchable PEDOT:PSS-based printed electrochemical device.[29] However, PEDOT:PSS is expensive, finds limited use as an electrode material in electrochemical devices, and could withstand strain of up to 100%.

In the present Letter, we leverage low-cost screen printing technology (Figure 1A) for large-scale fabrication of printable CNT-based electrochemical array devices that offer the highest stretchability reported to date by a printed device (Figure 1B). An important novel aspect of the present work is the judicious preparation of a highly stretchable CNT-based ink and its combination with judiciously designed device pattern that provides the device with two degrees of stretchability to accommodate extreme strains of upto 500%. Specifically, the device comprises of free-standing serpentine interconnects printed using stretchable CNT and Ag/AgCl inks (Figure 1B). Detailed experiments were performed to optimize the ink composition and connecting angle of the interconnects to obtain a printed device with highest stretchability. When an external strain is applied to the device, the serpentine structure unwinds to accommodate the stress (Figure 1C). Upon further increment of the applied load, the intrinsic stretchability of the printed ink – imparted by combining CNT with elastomeric polyurethane (PU) binder – offers additional stretchability to the device. Unlike their metallic counterparts,[11] the printed free-standing serpentine structures have two levels of stretchability – due to unwinding of free-standing serpentine structure (1st degree stretchability) and due to intrinsic stretchability of printable inks based on their tailored

formulation (2nd degree stretchability). This enables the CNT-based printed device to display remarkable stretchability compared to an earlier study.[29] CNT was selected as the electrode material since carbon is the most widely used electrode material due to its low background current, wide potential window, and electrochemical inertness.[30] Additionally, the functional groups present on the CNTs can be used to tether biomolecules or chemical moieties for specific sensing[31] and energy[32,33] applications without compromising their inherent stretchability. Furthermore, the exceptional mechanical and electrical properties of CNTs combined with the elastomeric properties of PU offer an attractive nanomaterial-based system for achieving stretchable electronic devices. To demonstrate the viability of the new platform to realize wide range of highly stretchable electrochemical sensors and biofuel cells, the CNT-based printed device array was employed for developing amperometric glucose sensor, an ion-selective ammonium ion potentiometric sensor, and enzymatic glucose biofuel cell. Coverage of these printable devices with different reagent layers does not compromise their resistance to extreme mechanical strains.

Intrinsic stretchability was achieved by utilizing specially synthesized intrinsically stretchable inks. As reported in our earlier work, commercial screen printable inks cannot be utilized to obtain stretchable devices due to the rigid nature of the patterns printed using these inks.[29] Hence, our efforts were directed towards preparing customized stretchable CNT and Ag/AgCl-based screen printable inks. Initially, varying amounts of CNTs were directly dispersed in Ecoflex® to obtain a stretchable CNT ink. However, a stretchable CNT ink with optimal printability, stretchability and electrochemical properties could not be achieved. Homogenous dispersion of conductive fillers within the binder is an essential requirement to obtain printable inks that demonstrate excellent printability and electrochemical response.[19] Keeping this in view, PU was considered as the stretchable binder due to its ability to form hydrogen bonds with the carboxyl groups of the CNTs, thus leading to improved dispersion of CNTs within the PU binder.[34] However, preliminary efforts of direct mixing of varying amounts of CNTs in PU led to inks possessing poor mechanical resiliency, high resistivity or sub-optimal electrochemical properties. This could be attributed to the unstable dispersion of CNTs in THF (Figure S1A) which affects the final dispersion of CNTs upon adding PU to obtain stretchable CNT ink. In order to address this challenge, suitable dispersing agents such as ionic liquid (1-ethyl-3-methylimidazolium tetrafluoroborate) and mineral oil were considered. Ultimately, mineral oil was chosen since it is inexpensive and led to homogenous dispersion of CNT in THF (Figure S1B). PU was then dispersed in the CNT-mineral oil suspension to obtain stretchable CNT ink that could be printed easily to fabricate conductive electrodes possessing excellent electrochemical and mechanical properties. Figure S2 shows SEM images of a stretchable CNT ink-based printed trace. The images indicate homogeneous distribution of CNTs within the PU and mineral oil matrix and the uniformity of the printed trace. The stretchable Ag/AgCl ink was prepared based on our earlier work.[29]

In order to achieve the goal of highly stretchable devices, an approach that relies on the synergistic effect of combining intrinsically stretchable screen printable inks and distinct design pattern that offers additional stretchability to the printed device was employed. The device-induced stretchability was achieved by designing interconnects between the active electrodes and contact pads in the form of free-standing serpentine structures with optimal

connecting angle. Several groups have shown that serpentine interconnects offer high levels of stretchability.[35,36] As depicted in Figure 1C, when an external load is applied to the printed device array, the free-standing serpentine interconnects accommodate most of the stress by unwinding themselves (1st degree stretching). This continues till the serpentine structures are almost straightened. Upon further increment of the applied strain, the intrinsic stretchability of the printed inks comes into play to offer further compliance to the applied stress (2nd degree stretching). Thus, the synergistic effect of device design and stretchable inks provides the printed device array with high tolerance towards extreme levels of multi-dimensional complex strains, as shown in Video V1 (supporting information). Images of the stretchable device array (Figure 1D) under various forms of mechanical deformations, including linear stretching, torsional twisting and indentation stress, are also shown in Figure 1E-G, respectively. The video and the images underscore the ability of the printed device array to endure extreme and complex multi-dimensional strains with minimal effect on its structural integrity.

Earlier reports on stretchable serpentine structures have revealed that parameters like inner radius (R), trace width (W) and connecting angle (θ) play an important role in dictating the extent of stretchability for the serpentine structures (Figure 1C, top right).[35,36] In order to obtain a compact device size, ‘R’ and ‘W’ were maintained at 2 mm and 1 mm, respectively, while ‘θ’ was varied between 0° to 45° to identify the best configuration that offers highest stretchability without compromising the structural integrity of the device. The extent of 1st degree stretching (unwinding of serpentine trace till it straightens) could be increased from ~57% to ~233% by changing ‘θ’ between 0 and 45°. Thus, geometrically, the stretchability of the device should increase with an increase in ‘θ’. Single free-standing Ag/AgCl serpentine traces of varying ‘θ’ were fabricated (Figure S3A) and changes in their resistance as a function of applied strain were recorded. As expected, serpentine structures with higher ‘θ’ values offer higher resiliency towards applied strain (Figure 2A). However, this was true only for ‘θ’ values from 0-30°. The serpentine with θ = 45° displayed poorer compliance towards mechanical deformations as compared to that with θ = 30°. This may be attributed to the fact that the serpentine structure with θ = 45° experiences complex out-of-plane bending and twisting while the external load is gradually removed. Out-of-plane bending and twisting of the serpentine structure leads to undesired strain at the microscopic level and thus causes an increase in resistance. Inferior resiliency of serpentine structures with θ = 45°, compared to that with θ = 30° towards external load has also been reported earlier.[36]

We also carried out experiments comparing free-standing serpentine traces fabricated using stretchable Ag/AgCl (Figure 2B) and CNT (Figure 2C) inks with corresponding stretchable ink-based surface-bound serpentine traces and with free-standing traces fabricated using non-stretchable Ag/AgCl (without Ecoflex binder) and CNT (without PU binder) inks. Schematics showing the surface-bound and free-standing Ag/AgCl and CNT inks-based traces are shown in Figure S3 B-E. Optical and electron microscopic analysis of the non-stretchable CNT-based trace clearly illustrate microscopic and macroscopic cracks throughout the trace immediately upon curing (Figure S4A and B) due to the absence of a binder to withhold the CNTs. Furthermore, SEM images reveal that the traces printed using non-stretchable CNT ink have a rough, non-uniform surface morphology (Figure S4C) as compared to the uniform printability offered by its stretchable counterpart (Figure S2B). The

superior printability of the stretchable CNT ink, as compared to the non-stretchable ink, can be attributed to the presence of PU that acts as an efficient binder for uniform dispersion of the CNTs. On the other hand, the non-stretchable Ag/AgCl-based free-standing trace could be stretched up to a strain of 200% due to the unwinding of the serpentine structure. However, application of additional stress led to immediate cracking of the trace due to the lack of intrinsic ink stretchability (Figure S5A) while no cracking was observed for the stretchable Ag/AgCl ink-based trace (Figure S5B). In the case of stretchable Ag/AgCl and CNT ink-based traces, stretched upto 500% strain, the resistance increased by ~800% and ~3500% for surface-bound Ag/AgCl and CNT-based devices, respectively, and by ~200% and ~ 300% for the free-standing Ag/AgCl and CNT-based free-standing traces. SEM studies analyzing the CNT-based free-standing trace before and after the 500% stretching reveal that initially the trace comprises of a crack-free homogenous morphology (Figure S6A). However, after application of 500% strain, microscopic cracks appear at some locations (Figure S6B). The microscopic cracks observed in the SEM images help explain the increased resistance of the printed traces upon undergoing mechanical deformations. It must be noted, however, that though the resistance increases, application of such extreme strains had a negligible impact on the electrochemical properties of the printed device (as discussed later and shown in Figures 3 and 4). As clearly evidenced from Figures 2B and C, the traces possessing single degree of stretchability display inferior stretchable property as compared the corresponding ones that have two degrees of stretchability. These data support the significance of traces possessing two degrees of stretching over their counterparts having single degree stretching (intrinsic stretchability or design stretchability), reflecting the former's ability to endure higher stretchability than that of the latter. Based upon these results, free-standing serpentine interconnects having $\theta = 30°$ were selected to realize the stretchable electrochemical device array.

Cyclic voltammetry is widely used to study different electrode materials and analyze changes in the electrode-electrolyte interface.[37] Hence, this technique was utilized to study the effect of applied strain on the electrochemical properties of the printed device array with ferricyanide as a redox probe. The first set of experiment comprised of studying the effect of increasing strain levels on cyclic voltammograms (CVs). The printed device was repeatedly stretched with increasing strains upto 500% (Figure 3A). The CV was first measured for an unstretched device (Figure 3A, black plot). It was later stretched to 100% of its length and then subsequently released to its initial position. This fatigue cycle was repeated 30 times and a CV was recorded. Similar fatigue cycles of increasing strains (upto 500%) were subsequently applied to the same device and the CV was measured at each step. The final CV recorded after 500% stretching is showing in Figure 3A (red plot). Stains >500% could not be applied since this pushed the underlying Ecoflex substrate (75 μm thickness) beyond its natural strain limits and led to its tearing. The device stretchability can be further improved by employing a thicker underlying substrate and by exploring other elastomers that offer stretchability greater than Ecoflex. As observed in Figure 3B, the redox peak separation (ΔE_p) as well as the peak heights of the ferricyanide probe remain nearly identical even when the device experiences such extreme levels of applied strains (R.S.D. for ΔE_p = 2.71%). These data indicate the minimal effect of severe mechanical deformations on the electrochemical properties of the printed device. The device can accommodate significantly

higher levels of strains than the device reported in our previous work (maximum strain: 100%)[29] due to its synergistic effect of intrinsic and design-induced stretchability. Furthermore, unlike the PEDOT:PSS electrodes used earlier, the current device rely on commonly used CNTs. The narrow peak separation and low background charging current, observed in the CVs of Figure 3, highlight the advantages of the CNT-based stretchable electrodes for electrochemical applications. Thereafter, the next study aimed at evaluating the effect of repeated stretching (300%) on the CVs obtained from the device. In this case, the device was stretched by 300% for total of 150 times and CVs were recorded after every 30 cycles. Figure 3C shows the initial (before stretching) and the final CV recorded at the end of the study The test again revealed that the device could easily withstand repeated stress cycles with negligible effect on its electrochemical properties (R.S.D. for ΔE_p = 2.30%).

Numerous real-life applications of stretchable devices mandate flawless performance even when the devices are continuously strained for extended periods. To analyze the performance of the printed device under such conditions, it was continuously maintained at a strain of 300% and the CV was recorded every 10 min (initial and final CVs are shown in Figure 3D). As evidenced from the figure, the CV shape remains almost similar over the entire test (R.S.D. for ΔE_p = 0.72%). Such real-time investigation of the device discloses its immaculate performance even when subjected to continuous stress of extreme levels. Again, it must be noted that the two levels of stretchability of the present device (shown in Figure 1C) allow it to offer a superior performance under continuous strain as compared to our earlier reported device (that could be maintained at 25% strain for a similar study).[29] The device was also tested for its defiance against complex, multi-dimensional deformations, for example, repeated indentations of 5 mm depth (Figure 1G) and repeated torsional twisting (Figure 1F). The initial and final CVs obtained during these experiments are shown in Figure 3E and F. These plots reveal that such multi-dimensional deformations also have minimal effect on the device's electrochemical properties (R.S.D. for ΔE_p = 3.45% and 0.95% for Figures 3E and F, respectively). Intermediate CVs recorded for the experiments depicted in 3**B-F** are shown separately in Figure S7.

Potentiometric ion-selective sensors and amperometric biosensors play a pivotal role in various healthcare[38,39] and environmental[40,41] applications. Several such applications mandate devices that can endure mechanical stress.[42] Hence, in such scenarios, the highly stretchable CNT-based device arrays can have immense use. Additionally, each CNT electrode of the array can be functionalized with specific receptor (e.g., ionophore or enzyme), thus offering multi-analyte detection. Considering such potential widespread applications, the CNT-based stretchable device was functionalized with an ammonium ion selective membrane as a proof-of-concept highlighting the utility of the new platform to realize highly stretchable potentiometric sensors (Figure 4A). The stretchable ammonium ion sensor displayed inconsequential effect of repeated 300% stretching on its potential response to varying ammonium concentrations (Figure 4B). During the entire mechanical resiliency study the sensor responded in a near-Nernstian fashion (67.5 mV/p[NH_4^+]) and its response fluctuated negligibly (RSD: 2.46 %), as observed in Figure 4C.

Similarly, the CNT-based device was functionalized with glucose oxidase (GOx) to demonstrate the ability of the stretchable platform in realizing highly stretchable amperometric biosensors. The glucose sensor was fabricated by functionalizing the CNT electrode with tetrathiafulvalene (TTF) as a mediator and GOx as the enzyme (Figure 4D). The resulting amperometric sensor displayed a linear response to increasing glucose levels (Figure 4E) along with negligible variance in its response when it was stretched repeatedly by 300% (Figure 4F, RSD: 4.98%).

Enzymatic biofuel cells, as energy harvesters and self-powered sensors, have garnered a tremendous recent attention for various invasive,[43,44] minimally invasive[45] and non-invasive,[46,47] applications. In such cases, the biofuel cells are intimately in contact with soft tissues that may undergo extreme mechanical deformations. The CNT-based stretchable device was thus modified to obtain a glucose biofuel cell. Specifically, the bioanode was functionalized with 1,4-naphthoquinone (NQ) as a mediator and GOx as the enzyme while the cathode comprised of electrodeposited platinum (Figure 4G). Figure 4H shows the power density (P.D.) curves obtained for increasing levels of glucose while Figure 4I shows the high stability of the power generated upon stretching the device repeatedly by 300% (RSD: 2.57%). The linear increase of the highest P.D. obtained from the stretchable biofuel cell with increasing glucose concentration (Figure 4H, inset) reveals that the biofuel cell also behaves as a self-powered glucose sensor. Such self-powered sensors are quite attractive for decentralized applications where powering sensors is a challenge.[48,49]

The results obtained from the potentiometric ammonium ion sensor, amperometric glucose sensor and enzymatic glucose biofuel cell and self-powered glucose sensor, underpins a compelling evidence of the ability of the stretchable CNT-based device array to be easily functionalized with a host of receptors and reagents to realize a wide range of highly stretchable electrochemical sensors and biofuel cells for diverse applications which demand intimate contact with surroundings and where extreme mechanical deformations are common. Furthermore, the results highlight that the device’s mechanical resiliency remains uncompromised even after coating it with layers containing delicate chemical and biochemical reagents. The array system can thus be utilized to realize highly stretchable multi-analyte sensors, multi-fuel biofuel cells, or a combination of sensors and biofuel cells.

In conclusion, the present work demonstrates the first example of a highly stretchable all-printed CNT-based electrochemical sensors and biofuel cells that can withstand strains as high as 500% with negligible effect on their structural integrity and electrochemical performance. The device thus offers the highest stretchability among all the reported screen printed devices. The printed device can endure such extreme stress due to the synergistic effects of its design pattern and use of specially engineered stretchable inks that offer stretchability at two levels – unwinding of the free-standing serpentine interconnects and intrinsic stretchability of custom-designed inks which rely on the exceptional mechanical and electrical properties of CNTs and elastomeric properties of PU binder. The device has been characterized using resistance and various electroanalytical techniques for studying its mechanical deformation resiliency. Preliminary resistance studies reveal the pivotal role played by free-standing serpentine interconnects and control of their connecting angle in realizing the high stretchability. Subsequent CV studies indicate that the device shows

negligible variation in its electrochemical response even when repeatedly stretched (up to 500%), twisted and indented. The device also performed flawlessly when continuously stretched by 300% for 1h. As compared to previous work on PEDOT:PSS based printed stretchable device,[29] the present device relies on commonly used CNT electrodes and demonstrates superior stretchability. Ultimately, the CNT-based device was functionalized with reagent layers containing ionophores or enzymes to realize highly stretchable ammonium ion-selective potentiometric sensor, amperometric glucose biosensor and enzymatic glucose biofuel cell and self-powered biosensor. The sensors and biofuel cells displayed remarkable endurance towards repeated strains of 300%, indicating minimal effect of applied stress on the electrode material and also on delicate enzymes and other reagents immobilized onto the electrodes. Furthermore, CNT-based electrodes represent a common platform that allows wide range of strategies to immobilize receptors and other reagents into highly bio-compatible three dimensional micro-environments to realize sensors and biofuel cells with improved characteristics.[50,51] The array system thus offers the opportunity to fabricate multi-analyte sensors, multi-fuel biofuel cells and a combination of sensors and biofuel cells, thus providing a multi-functional platform for sensing and energy harvesting. Future work will focus on further characterizing the inks' rheological properties, studying the tensile properties of the printed traces and the performance of the device while undergoing dynamic repeated large strain, and on improving further the stretchability (beyond 500%) by employing thicker substrates and exploring other highly stretchable elastomers. The present work therefore has the promise to lay the foundation for scalable, low-cost fabrication of fully-printed highly stretchable and high-performance electrochemical devices for diverse applications in healthcare, defense, consumer electronics and energy domains.

Supplementary Material

Refer to Web version on PubMed Central for supplementary material.

Acknowledgements

This work was supported by the NIH (Award R21EB019698) and ARPA-e (Award DE-AR0000535). A.J.B., I.J. and R.N.F. acknowledge support from Siebel Scholars Foundation, the Thai Development and Promotion of Science and Technology Talented Project (DPST), and the UCSD Initiative for Maximizing Student Diversity (IMSD), respectively.

References

1. Kim DH, Ghaffari R, Lu NS, Rogers JA. Annu Rev Biomed Eng. 2012; 14:113–128. [PubMed: 22524391]
2. Lipomi DJ, Bao ZA. Energ Environ Sci. 2011; 4:3314–3328.
3. Ramuz M, Tee BCK, Tok JBH, Bao ZN. Adv Mater. 2012; 24:3223–3227. [PubMed: 22641411]
4. Cotton DPJ, Graz IM, Lacour SP. Ieee Sens J. 2009; 9:2008–2009.
5. Kaltenbrunner M, Sekitani T, Reeder J, Yokota T, Kuribara K, Tokuhara T, Drack M, Schwodiauer R, Graz I, Bauer-Gogonea S, Bauer S, Someya T. Nature. 2013; 499(7459):458. [PubMed: 23887430]
6. Lu N, Kim DH. Soft Robotics. March. 2014; 1:53–62.
7. Majidi C. Soft Robotics. March. 2014; 1:5–11.
8. Someya T. Ieee Spectrum. 2013; 50:50–56.

9. Kim J, Lee M, Shim HJ, Ghaffari R, Cho HR, Son D, Jung YH, Soh M, Choi C, Jung S, Chu K, Jeon D, Lee ST, Kim JH, Choi SH, Hyeon T, Kim DH. Nat Commun. 2014:5.
10. Rogers JA, Someya T, Huang YG. Science. 2010; 327:1603–1607. [PubMed: 20339064]
11. Xu S, Zhang YH, Cho J, Lee J, Huang X, Jia L, Fan JA, Su YW, Su J, Zhang HG, Cheng HY, Lu BW, Yu CJ, Chuang C, Kim TI, Song T, Shigeta K, Kang S, Dagdeviren C, Petrov I, Braun PV, Huang YG, Paik U, Rogers JA. Nat Commun. 2013; 4:1543. [PubMed: 23443571]
12. Takahashi T, Takei K, Gillies AG, Fearing RS, Javey A. Nano Lett. 2011; 11(12):5408–5413. [PubMed: 22050705]
13. Gong S, Schwalb W, Wang YW, Chen Y, Tang Y, Si J, Shirinzadeh B, Cheng WL. Nat Commun. 2014; 5:3132. [PubMed: 24495897]
14. Savagatrup S, Printz AD, Rodriquez D, Lipomi DJ. Macromolecules. 2014; 47:1981–1992.
15. Gong S, Lai DTH, Wang Y, Yap LW, Si KJ, Shi Q, Jason NN, Sridhar T, Uddin H, Cheng W. ACS Appl. Mater. Interfaces. 2015; 7:19700–19708. [PubMed: 26301770]
16. Kubo M, Li XF, Kim C, Hashimoto M, Wiley BJ, Ham D, Whitesides GM. Adv Mater. 2010; 22:2749–2752. [PubMed: 20414886]
17. Kim DH, Lu NS, Ma R, Kim YS, Kim RH, Wang SD, Wu J, Won SM, Tao H, Islam A, Yu KJ, Kim TI, Chowdhury R, Ying M, Xu LZ, Li M, Chung HJ, Keum H, McCormick M, Liu P, Zhang YW, Omenetto FG, Huang YG, Coleman T, Rogers JA. Science. 2011; 333:838–843. [PubMed: 21836009]
18. Akter T, Kim WS. Acs Appl Mater Inter. 2012; 4:1855–1859.
19. Metters JP, Kadara RO, Banks CE. Analyst. 2011; 136:1067–1076. [PubMed: 21283890]
20. Kamyshny A, Magdassi S. Small. 2014; 10:3515–3535. [PubMed: 25340186]
21. Carrilho E, Martinez AW, Whitesides GM. Anal Chem. 2009; 81:7091–7095. [PubMed: 20337388]
22. Chen PC, Chen HT, Qiu J, Zhou CW. Nano Res. 2010; 3:594–603.
23. Bandodkar AJ, O'Mahony AM, Ramirez J, Samek IA, Anderson SM, Windmiller JR, Wang J. Analyst. 2013; 138:5288–5295. [PubMed: 23865089]
24. Cunningham JC, Brenes NJ, Crooks RM. Anal Chem. 2014; 86:6166–6170. [PubMed: 24871788]
25. Kim J, Valdes-Ramirez G, Bandodkar AJ, Jia WZ, Martinez AG, Ramirez J, Mercier P, Wang J. Analyst. 2014; 139:1632–1636. [PubMed: 24496180]
26. Cai J, Cizek K, Long B, McAferty K, Campbell CG, Allee DR, Vogt BD, La Belle J, Wang J. Sens. Actuators B. 2009; 137:379–385.
27. Schazmann B, Morris D, Slater C, Beirne S, Fay C, Reuveny R, Moyna N, Diamond D. Anal Methods-Uk. 2010; 2:342–348.
28. Chuang MC, Windmiller JR, Santhosh P, Ramirez GV, Galik M, Chou TY, Wang J. Electroanalysis. 2010; 22:2511–2518.
29. Bandodkar AJ, Nunez-Flores R, Jia WZ, Wang. J. Adv Mater. 2015; 27:3060–3065.
30. Wang J. Electroanal. 2005; 17:7–14.
31. Merkoci A, Pumera M, Llopis X, Perez B, del Valle M, Alegret S. Trac-Trend Anal Chem. 2005; 24:826–838.
32. Zhou M, Deng L, Wen D, Shang L, Jin LH, Dong SJ. Biosens Bioelectron. 2009; 24:2904–2908. [PubMed: 19321330]
33. Liu XM, Huang ZD, Oh SW, Zhang B, Ma PC, Yuen MMF, Kim JK. Compos Sci Technol. 2012; 72:121–144.
34. Sahoo NG, Jung YC, Yoo HJ, Cho JW. Macromol. Chem. Phy. 2006; 207:1773–1780.
35. Gonzalez M, Axisa F, BuIcke MV, Brosteaux D, Vandevelde B, Vanfleteren. J. Microelectron Reliab. 2008; 48:825–832.
36. Carta R, Jourand P, Hermans B, Thoné J, Brosteaux D, Vervust T, Bossuyt F, Axisa F, Vanfleteren J, Puers R. Sens. Actuators A. 2009; 156:79–87.
37. Wang, J. Analytical Electrochemistry. New York: Wiley; 2006.
38. Miller PR, Xiao XY, Brener I, Burckel DB, Narayan R, Polsky R. Adv Healthc Mater. 2014; 3:876–881. [PubMed: 24376147]

39. Rose DP, Ratterman ME, Griffin DK, Hou LL, Kelley-Loughnane N, Naik RR, Hagen JA, Papautsky I, Heikenfeld JC. Ieee T Bio-Med Eng. 2015; 62:1457–1465.
40. Hart JP, Wring SA. Trac-Trend Anal Chem. 1997; 16:89–103.
41. O'Mahony AM, Windmiller JR, Samek IA, Bandodkar AJ, Wang. J. Electrochem Commun. 2012; 23:52–55.
42. Bandodkar AJ, Molinnus D, Mirza O, Guinovart T, Windmiller JR, Valdes-Ramirez G, Andrade FJ, Schoning MJ, Wang J. Biosens Bioelectron. 2014; 54:603–609. [PubMed: 24333582]
43. Halamkova L, Halamek J, Bocharova V, Szczupak A, Alfonta L, Katz E. J Am Chem Soc. 2012; 134:5040–5043. [PubMed: 22401501]
44. Szczupak A, Halamek J, Halamkova L, Bocharova V, Alfonta L, Katz E. Energ Environ Sci. 2012; 5:8891–8895.
45. Valdes-Ramirez G, Li YC, Kim J, Jia WZ, Bandodkar AJ, Nunez-Flores R, Miller PR, Wu SY, Narayan R, Windmiller JR, Polsky R, Wang J. Electrochem Commun. 2014; 47:58–62.
46. Jia W, Valdés-Ramírez G, Bandodkar AJ, Windmiller JR, Wang J. Angew. Chem. Int. Ed. 2013; 52:7233–7236.
47. Jia W, Wang X, Imani S, Bandodkar AJ, Ramirez J, Mercier PP, Wang J. J. Mater. Chem. A. 2014; 2:18184–18189.
48. Hahn, R.; Reichl, H. Batteries and power supplies for wearable and ubiquitous computing; Proceedings of the 3rd International Symposium on Wearable Computers; Oct 18-19, 1999; San Francisco, USA.
49. Zhou M. Electroanalysis. 2015; 27:1786–1810.
50. Li L, Wang Y, Pan L, Shi, Cheng W, Shi Y, Yu G. Nano Lett. 2015; 15:1146–1151. [PubMed: 25569673]
51. Zhai D, Liu B, Shi Y, Pan L, Wang Y, Li W, Zhang R, Yu G. ACS Nano. 2013; 7:3540–3546. [PubMed: 23472636]

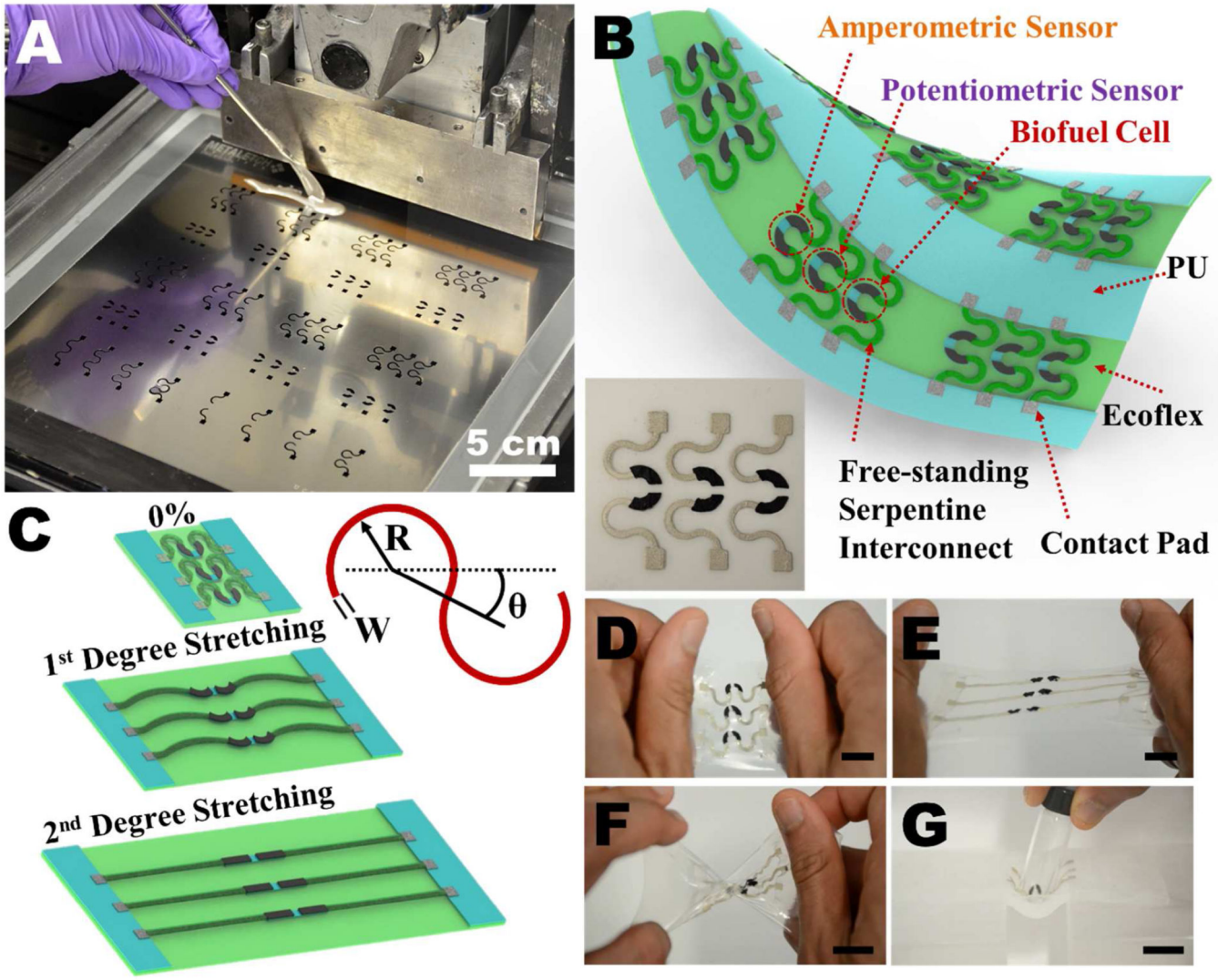

Figure 1.

(A) Image of the stencil employed for printing the stress-enduring stretchable devices. Schematics showing **(B)** large-scale printed stretchable device arrays along with their various applications (Inset shows an image of a printed CNT-based array device) and **(C)** the two degrees of stretching – design-induced (1st Stretching) and intrinsic stretchability (2nd Stretching) – enabling the printed arrays to accommodate high levels of strains along with parameters defining the curvature of a free-standing serpentine interconnect (top right). Photographs of stretchable array under **(D)** 0% and **(E)** 175% linear **(F)** 180° torsional and **(G)** 5 mm indention strains. Scale bar for images D-G, 1cm.

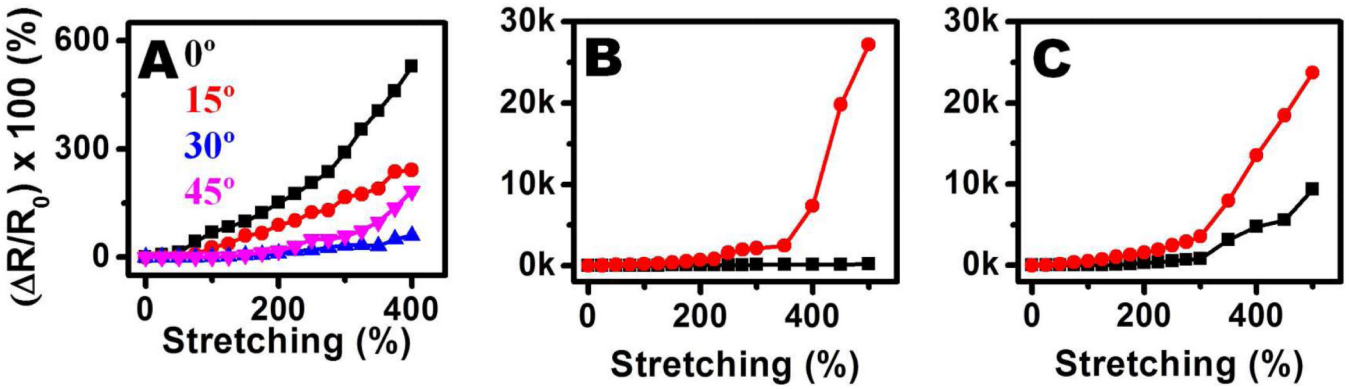

Figure 2.

Comparison of the effect of applied strain on the resistance of printed **(A)** free-standing Ag/AgCl-based trace possessing different contacting angles (θ); **(B)** Ag/AgCl-based free-standing (black plot) and surface-bound (red plot) serpentine traces (θ = 30°) and **(C)** CNT-based free-standing (black plot) and surface-bound (red plot) serpentine traces (θ = 30°).

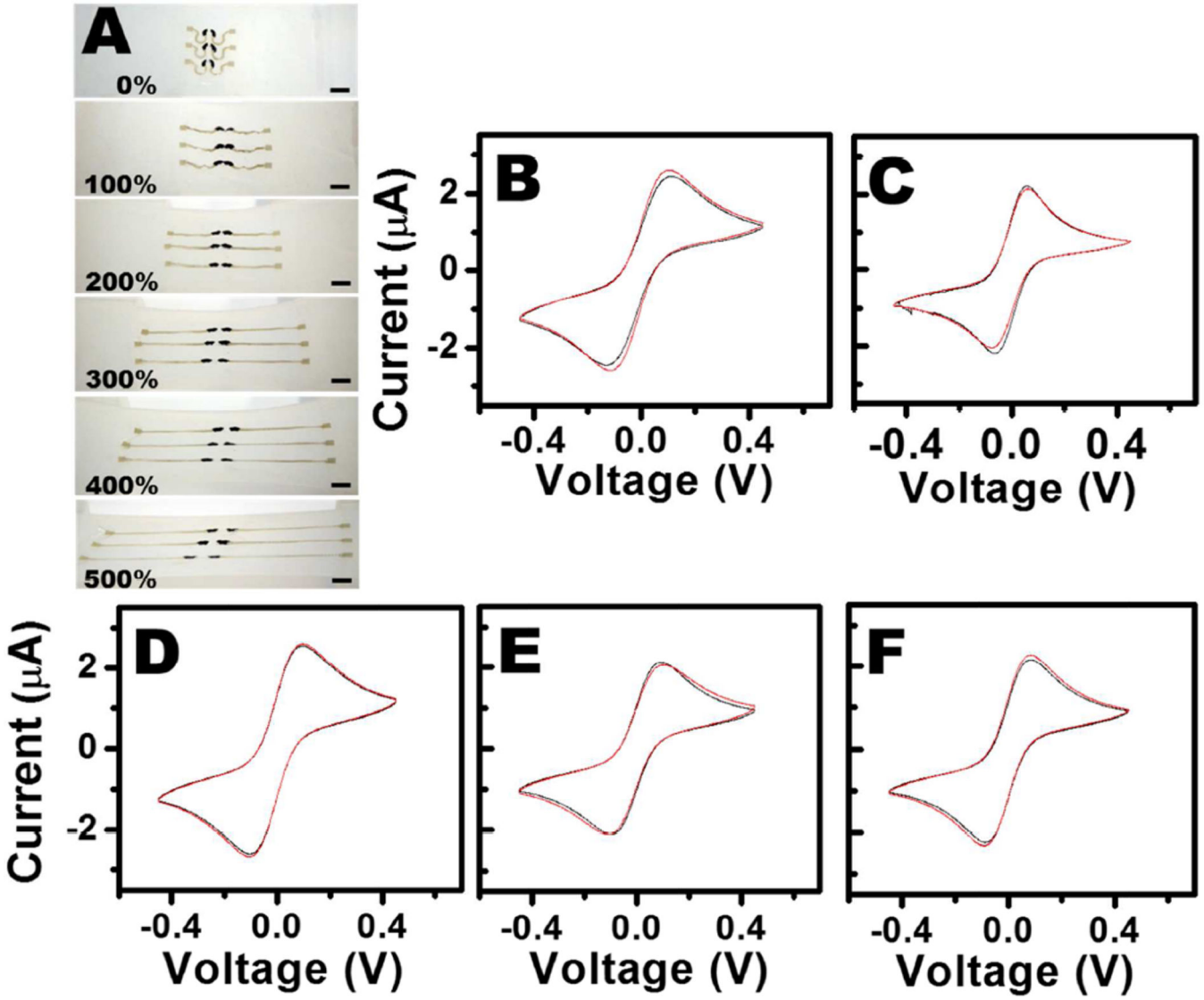

Figure 3.

(A) Photographs of the printed stretchable array under increasing levels of applied strain (scale bar = 1cm). CVs recorded before (black plot) and after (red plot) applying **(B)** increasing levels of strain from 0 to 500% with increments of 100%, **(C)** repeated 300% stretching cycles for a total of 150 iterations, **(D)** a continuous strain of 300% for 60 min, and after applying **(E)** repeated indentations (5 mm) for a total of 50 repetitions and **(F)** repeated torsional twisting stress cycles for a total of 50 iterations. (**B, C, E and F**): The device was maintained at maximum strain for 2 s during each stress cycle. Corresponding intermediate CVs recorded for **B-F** are shown in Figure S7.

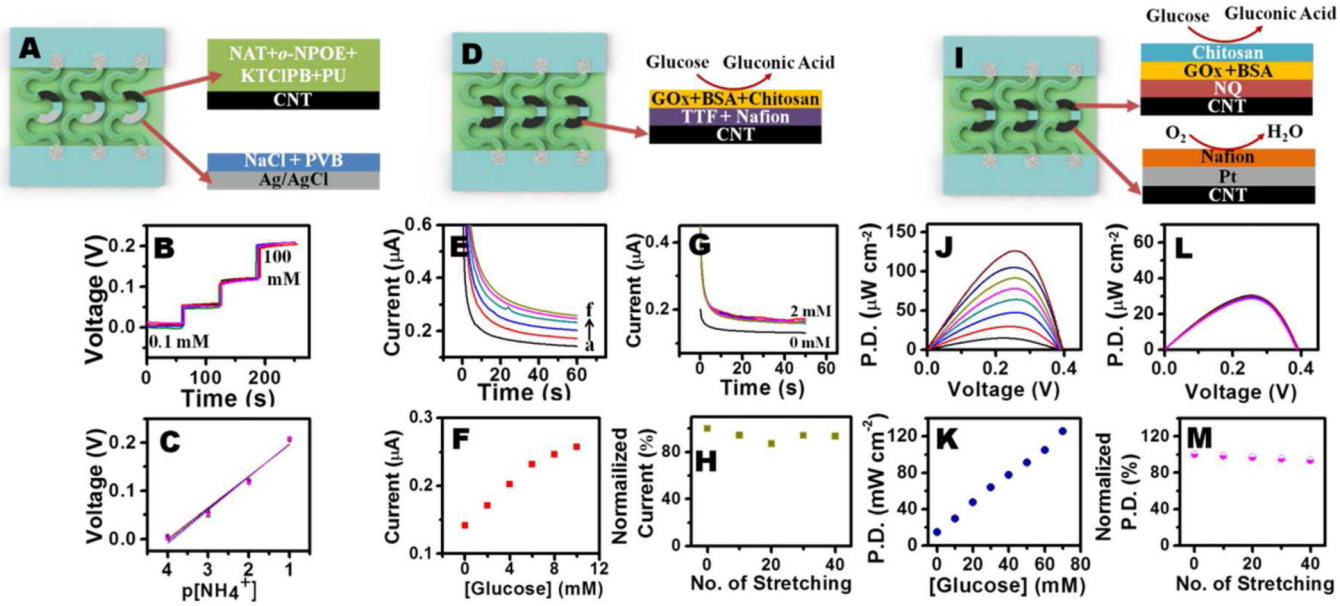

Figure 4.

(A) Schematic of a stretchable ion-selective NH_4^+ sensor. **(B)** Voltage vs time data recorded for increasing NH_4^+ concentration (0.1 – 100 mM) and **(C)** Calibration plot recorded after application of 10 cycles of 300% strain for a total of 40 cycles. **(D)** Schematic of a stretchable amperometric glucose sensor. **(E)** Amperograms recorded for increasing glucose concentration (a –f: 0 – 10 mM). **(F)** Corresponding calibration plot. **(G)** Amperograms obtained for a glucose sensor after every 10 cycles of 300% stretching for a total of 40 iterations and **(H)** stability of the sensor response after each 300% stretching iterations. **(I)** Schematic of a stretchable glucose bio-fuel cell. **(J)** Power density vs voltage curves for the stretchable glucose bio-fuel cell and **(K)** maximum power density vs glucose concentration. **(L)** Power density vs voltage plots for a glucose bio-fuel cell after every 10 cycles of 300% stretching for a total of 40 iterations and **(M)** biofuel cell stability after each 300% stretching iterations. (**B, G and L**): The device was maintained at maximum strain for 2 s during each stress cycle.